Contents lists available at ScienceDirect

Bioresource Technology

Thermophilic bio-electro carbon dioxide recycling harnessing renewable energy surplus

Laura Rovira-Alsina, M. Dolors Balaguer, Sebastià Puig [*]

LEQUiA, Institute of the Environment, University of Girona, Campus Montilivi, C/Maria Aurèlia Capmany, 69, E-17003 Girona, Catalonia, Spain

HIGHLIGHTS

- Renewable energy surplus can be valorized through microbial electrosynthesis.
- Intermittent power supply conditions may boost the product per energy ratio.
- Enriched thermophilic microbiomes can be highly resilient to fluctuating conditions.
- (Bio)electrochemical processes co-exist with fermentative reactions.

GRAPHICAL ABSTRACT
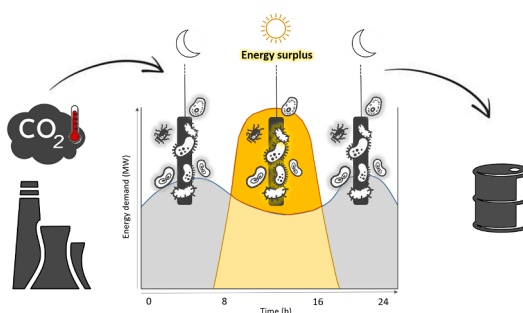
ABSTRACT

Renewable energies will represent an increasing share of the electricity supply, while flue and gasification-derived gases can be a promising CO_2 feedstock with a heat load. In this study, microbial electrosynthesis of organic compounds from CO_2 at high temperature was proposed as an alternative for valorising energy surplus and decarbonizing the economy. The unremitting fluctuation of renewable energy sources was assessed using two bioreactors at 50 °C, under circumstances of continuous and intermittent power supply (ON-OFF; 8–16 h), simulating an off-grid photovoltaic system. Results highlighted that maximum acetate production rate (43.27 g m^{-2} d^{-1}) and columbic efficiency (98%) were achieved by working with an intermittent energy supply, while current density was reduced three times. This boosted the production of acetate per unit of electricity provided up to 138 g kWh^{-1} and reinforced the robustness of the technology by showing resilience to tolerate perturbations and returning to its initial state.

1. Introduction

Renewable energy has emerged as a progressive step to reach a sustainable energy economy (WEO, 2018). Not only using environmentally friendly energy, but also employing it much more efficiently (Denchak, 2018). However, since these sources are hampered by a discontinuous output of energy, the problem in balancing supply and demand is still not fully solved (Anvari et al., 2016). 4 out of 27 countries of the European Member States reported a deficit of renewable energy in 2018 (European Environment Agency, 2019), but 10 of them foresaw an expected excess by 2020. As an example, Spain overall surplus was estimated to account for 2,649 ktoe (30,808 MWh), (ECN,

2011). Photovoltaic (PV) installations generate a surplus of energy during approximately 8 h per day, coinciding with the solar peak hours (SPH) of this region (Spanish solar radiation data). This becomes more relevant in off-grid systems for isolated locations without reliance on public utilities. Seasonal storage of renewable energy surplus could connect economic and environmental gains by means of a circular and decarbonized economy approach. Hence, there is a need for seeking technologies other than conventional lithium-ion batteries able to collect, transport and convert excess energy (Hu et al., 2017).

Microbial electrosynthesis (MES) has been proposed as a technically feasible near-term technology for carbon dioxide (CO_2) application (Grim et al., 2020; Bian et al., 2020). Recently, Roy et al. (2021) stablished the first demonstration of microbial electrosynthesis from unpurified industrial CO_2. MES is based on electricity-driven microbial reactions to transform CO_2 from a liability into an asset, while converting excess renewable energy into chemical platforms (Nevin et al., 2010; Rabaey and Rozendal, 2010). Up to now, MES is rooted in the bioH$_2$-mediated production of organics, mainly acetate (Bian et al., 2020) or short-chain volatile fatty acids (Jourdin et al., 2019; Vassilev et al., 2019). The organics generated could be used as building blocks for other end-products (i.e. bioplastics (Pepè Sciarria et al., 2018)). The production of hydrogen (H_2), either biological or electro-catalytic, plays a key role in H_2-mediated biological reactions as it governs the availability of reducing power and the end-products (Blasco-Gómez et al., 2019; Puig et al., 2017). MES is expected to be an appropriate option for *in-situ* H_2 production and utilization. However, while CO_2 as the sole carbon source is suitable for autotrophic electroactive bacteria acting as catalysts, the intermittency of renewable energy as the only electron donor source could adversely influence the microbial community (Gowrisankaran et al., 2015) and thus, the overall performance of this technology.

Several mesophilic studies have been carried out assuming the use of renewable energy in MES (Ceballos-Escalera et al., 2019; Sánchez et al., 2019; Streeck et al., 2018). Nonetheless, only a few have determined the influence that continuous power supply interruptions could suppose on the stability of the process. Anzola Rojas and co-workers suggested a slight reduction in the production rates, or even shifts in the metabolic pathways that could alter the microbial structure, and provoke the cell death (Anzola Rojas et al., 2018b). They observed a decrease in the concentration of acetic acid during different disconnection time spans (from 4 to 64 h), assuming that it was oxidized back to CO_2 (Anzola Rojas et al., 2018a). Despite, there is a lack of knowledge on the influence of using exclusively the renewable energy surplus, and the prolonged effect of the daily repetition of periods with/without electrical connection at thermophilic conditions (above 40 °C).

Flue and gasification-derived gases have been postulated as a promising feedstock (Liu et al., 2020), containing a high percentage of CO_2 (10–30% *v/v*) compared to the atmospheric concentration (0.04% *v/v*). However, the usage of these carbon streams is limited by the high temperature. In our previous study, we demonstrated the ability of a mixed microbial electroactive culture to effectively produce H_2 and acetate from CO_2 mimicking saturated industrial effluent under long-term thermophilic conditions (Rovira-Alsina et al., 2020). The present work assesses the potential integration of thermophilic MES with renewable energy surplus. Two microbial electrolysis cells were operated at 50 °C for the bio-electro CO_2 recycling into organic compounds with repetitive cycles of intermittent power supply (ON-OFF; 8–16 h), simulating off-grid PV systems. H_2, CO_2 and organic compounds productions were monitored over time under conditions of biological stress, which could reflect a wide range of physical responses as a direct effect for homeostasis perturbation, moving forward the development of a robust and resilient microbial community.

2. Materials and methods

2.1. Experimental setups

Two MES systems named R1 and R2 were constructed. They consisted of two identical glass H-type bottles of 0.25 L (Pyrex V-65231 Scharlab, Spain), separated by a cation exchange membrane of $2 \cdot 10^{-4}$ m^2 (CMI-1875 T, Membranes international, USA). The cathode consisted of a plain carbon cloth (thickness of 490 μm, surface area of $3 \cdot 10^{-3}$; NuVant's Elat LT2400 FuelCellsEtc, USA) connected to a stainless-steel wire. The anode was a $2 \cdot 10^{-6}$ m^3 graphite rod of 0.1 m length and $5 \cdot 10^{-3}$ m of diameter (EnViro-cell, Germany). An Ag/AgCl electrode (+0.197 V *vs.* SHE, model RE-5B, BASI, UK) with an operating temperature range from 0 to 60 °C was placed in the cathodic chamber and used as a reference electrode. Reactors were sealed with butyl rubber caps to prevent gas leakage and keep the headspace volume of each chamber at 0.03 L, while liquid volume accounted for 0.22 L.

Both MES systems were operated in a three-electrode configuration with a potentiostat (BioLogic, Model VSP, France), which controlled the cathode potential at −0.6 V *vs.* SHE (standard hydrogen electrode) and monitored the current demand over time. All the potentials reported in this work are relative to SHE unless otherwise noted. Prior to use, the working electrodes were pre-treated in a 0.5 M solution of HCl and a 0.5 M of NaOH for a total of two days and rinsed with deionized water for an additional day. At the end of the experimental study, the voltage of the reference electrodes was measured to ensure any shift that may have occurred during operation. The temperature was kept constant at 50 °C using an orbital incubator (SI600 Stuart, UK), and an agitation rate of 80 rpm was fixed to enable mixing and facilitate mass transfer inside the cathodic chambers. The reactors were operated in batch mode and kept in the dark to avoid the growth of phototrophic microorganisms.

2.2. Inoculum

The microbial community was taken from an anaerobic digester working at 37.5 °C of a wastewater treatment plant (WWTP) located in Girona, Spain. A 1:20 dilution with synthetic medium based on ATCC1754 growth medium (Tanner et al., 1993) was incubated in 50 °C fermentative reactors under H_2:CO_2 (80:20 *v/v*) to promote acetogenesis and microorganisms' adaptation to thermophilic conditions. During this enrichment stage, pH was adjusted to 6.0 and 2-bromoethanesulfonic acid (10 mM) was added to prevent methanogenesis (Jadhav et al., 2018). An additional 1:10 dilution of this inoculum with the reformulated medium to remove all sources of organic carbon, was used to operate the reactors. The microbial community structure was analyzed in previous experiments (Rovira-Alsina et al., 2020), in which *Thermoanaerobacterales* was the dominant order. At the genus level, *Moorella* and *Caloribacterium* were the most representative. The experiment was carried out during a steady state phase of the both reactors (after 155 days of operation) so that no other variable interfered with the results.

2.3. Monitoring of key operating parameters

BioLogic software (EC-Lab v10.37) was used to alternatively run multi-technique electrochemical routines with the potentiostat, which included closed-circuit operation in chronoamperometry (CA) and open-circuit voltage (OCV). A cathode potential of −0.6 V was fixed for CA whereas its variation was followed during OCV. The general test lasted 5 consecutive weeks. Repetitive cycles of intermittent power supply were performed from week 2 to 4 (both included), while weeks 1 and 5 were used as controls working in CA mode. During weeks 2 to 4, electrical energy was supplied 8 h per day (CA mode), and it was disconnected the next 16 h (OCV mode). In both modes of operation, the cell voltage (E_{cell}) was recorded continuously except at the end of week 3, in which there was a general power outage. Pure CO_2 (99.9%, Praxair, Spain) was used to feed the two MES systems. Gas was sparged for 10 min in the

cathodic chamber once a week to oversaturate the liquid media and renew the headspace, whereas it was added punctually from 1 to 3 times per week to ensure carbon bioavailability. Gas bags (FlexFoil 301.44 Cromlab SL, Spain) were attached in the gas outlet during weekends, whilst during the week, gas pressure was maintained below 4 atm, releasing it to prevent liquid leakages. Samples from the liquid phase were taken from twice to ten times per week depending on the experimental period. The withdrawn liquid during sampling was replaced with freshly prepared medium saturated with CO_2 to maintain constant volumes in both chambers. Finally, 50 mL of fresh medium were added in R2 at day 15 of operation to evaluate the effect of mineral medium replacement. The initial pH of the solution was set at 6.0, but it was not further modified neither with acidic nor basic solutions.

2.4. Analyses and calculations

Conductivity and pH were measured with an electrical conductivity meter (EC-meter basic 30+, Crison, Spain) and a multimeter (Multi-Meter 44, Crison, Spain), respectively. Both devices were calibrated to measure at 50 °C. The concentration of organic compounds (volatile fatty acids and alcohols) in the liquid phase was determined using an Agilent 7890A gas chromatograph equipped with a DB-FFAP column and a flame ionization detector. Gas production was quantified in the MES by measuring the pressure in the headspace of the reactors using a digital pressure sensor (differential pressure gauge, Testo 512, Spain). Gas samples were analyzed periodically during experiments by gas chromatography (490 Micro GC system, Agilent Technologies, US). The GC was equipped with two columns: a CP-molesive 5A for methane (CH_4), carbon monoxide (CO), H_2, oxygen (O_2) and nitrogen (N_2) analysis, and a CP-Poraplot U for CO_2 analysis. The two columns were connected to a thermal conductivity detector (TCD).

The concentrations of dissolved H_2 and CO_2 in the liquid media were calculated using Henry's law at 50 °C (Eq. (1)), where C_i is the solubility of a gas in a particular solvent (mol L^{-1}), H_i is the Henry's law constant in mol L^{-1} atm^{-1} (0.0007 for H_2 and 0.0195 for CO_2; values taken from Foust et al. (1959) and recalculated based on the operational temperature using equations from Stumm and Morgan (1996)), and $P_{gas\ i}$ is the partial pressure of the gas in atm.

$$C_i = H_i A \cdot P_{gasi} \tag{1}$$

The columbic efficiency (CE) for the conversion of current into products (i.e. H_2, acetate, ethanol) was calculated weekly according to Patil et al. (2015) in CA mode (Eq. (2)). C_i is the compound i concentration in the liquid phase (mol C_i L^{-1}), n_i is the molar conversion factor (2, 8 and 18 mol_{eq}^{-1} for H_2, acetate and ethanol, respectively), F is the Faraday's constant (96485C mol e^{-1}), V_{NCC} is the net liquid volume of the cathode compartment (L), and I the current density of the system (A).

$$CE(\%) = \frac{C_i A \cdot \sum_i n_i A \cdot FA \cdot V_{NCC}}{\int_0^t IA \cdot dt} A \cdot 100 \tag{2}$$

Carbon conversion (CC) yield was calculated as the percent variation between the product formed depending on the converted CO_2 as stated in Eq. (3). ΔC_{CO2} is the difference of CO_2 in the gas plus liquid phases from the beginning (immediately after feeding the system) to the end of a batch, and $\Delta C_{products}$ is the difference of organic products (i.e. acetate) between batches.

$$CC(\%) = \frac{\Delta C_{products}}{\Delta C_{CO_2}} A \cdot 100 \tag{3}$$

The optical density (OD) of the bulk liquid was periodically measured to control the growth of the planktonic microbial community with a spectrophotometer (CE 1021, 1000 Series, CECIL Instruments Ltd., UK) at a wavelength of 600 nm. The dry cell weight (DCW) was calculated in g L^{-1} by interpolating the OD values in an experimental

regression line created using the corresponding mixed inoculum (1 OD = 0.57 g L^{-1} of DCW).

3. Results and discussion

A detailed monitoring of the main variables has been exposed along the following sections to evaluate the performance of the MES reactors. The results of operating the systems with only the surplus of photovoltaic renewable energy, therefore with repetitive cycles of intermittent power, has been described.

3.1. Current density and products unfolding to switching electrical conditions

Two replicate reactors (R1 and R2) were used to assess an alternative strategy of operation, based on following the daily cycle of sunlight with ON-OFF power supply periods (8 h ON vs. 16 h OFF). Fig. 1 presents the current density and cell voltage profiles of the reactors over time, discerning CA and OCV operation mode. Both reactors followed the same response to the electrical switching conditions. However, the current density of R2 was slightly higher compared to R1. This was linked to a greater increase in electroactivity from week 1, which led to a higher H_2 formation (Fig. 2). During continuous power supply (weeks 1 and 5) the current demand was stable, though peaks of higher intensity were associated to CO_2 feeding points (Batlle-Vilanova et al., 2019) and the accumulation of organics. However, during intermittent disconnection (weeks 2 to 4), shorter spikes could also be related to sudden energy inputs (Zhang et al., 2019). Throughout these weeks, current demand abruptly increased when electricity was connected and progressively decreased along with each CA period. When operated at OCV, the cathode potential rapidly tended to −0.5 V and stabilized in this value until the electric circuit was closed again. Concomitantly, the anode potential decreased up to 0.5 V, giving a theoretical applied cell voltage of 1 V (Fig. 1). The E_{cell} was gradually intensified throughout the weeks as a result of an increase of the ohmic resistance of the system (i.e. sacrificial anode), which came along with a higher current demand, reaching greater levels than when electricity was supplied uninterruptedly (weeks 1 and 5). For instance, maximum values of week 4 were 10.9 A m^{-2} for R1 and 13.2 A m^{-2} for R2, though in week 5 they decreased until 8.8 and 12.0 A m^{-2}, respectively.

Fig. 2 presents the evolution of total gas (GP) and H_2 partial pressures (P_{H2}), besides acetate concentrations of both reactors over time. H_2 was continuously produced throughout the experiment, which led to an H_2-mediated production of organics from electricity and CO_2. The first week of the experiment, organic concentrations and H_2 partial pressures were similar between reactors. Operating at CA mode (days −7 to 0), P_{H2} rapidly increased and could barely stabilize at 2 atm until the next batch. This was accompanied by a gradual increase in acetate concentration at a rate of 6.60 ± 0.73 g m^{-2} d^{-1}. The following 3 weeks (days 0 to 21), the systems operated at intermittent CA-OCV mode. This slightly affected the gas pressure evolution, which oscillated depending on the electric circuit position (open or closed). However, acetate continued accumulating at a similar rate compared to the first week (8.07 ± 3.67 g m^{-2} d^{-1}). Once the continuous electric supply was reestablished (days 21 to 28), the initial behavior of both systems was restored, showing similar H_2 partial pressures and organics profiles as the first week. The maximum acetic acid concentration (6.0 g L^{-1}) was achieved in R1, while H_2 and overall gas pressure turned out to be higher in R2 (maximum of 2.8 and 3.8 atm, respectively). Despite the experiments were carried out under identical operating conditions, a higher bulk density of R1 compared to R2 (0.12 vs. 0.08 g L^{-1}; DCW of Table 1), together with a lower cell voltage (3.9 vs. 8.5 V; Fig. 1), could have promoted a greater production of organic compounds.

Uninterrupted CA mode operation (weeks 1 and 5) usually induced to higher H_2 partial pressures compared to the combination of CA and OCV modes (weeks 2 to 4). Under CA operation, gas pressure increased
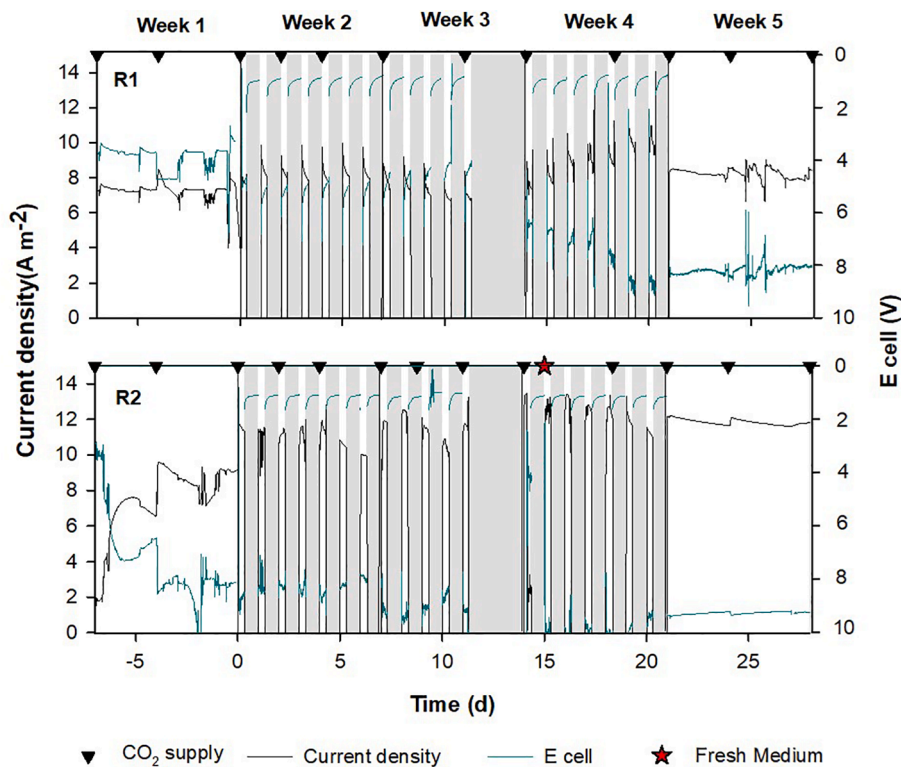
Fig. 1. Current density profiles (black line), and cell potential (Ecell; green line) over time in R1 and R2. White areas represent operation at CA mode, grey areas of OCV mode, black inverted triangles the CO$_2$ feeding points, red star when fresh medium was added, and vertical black lines separate the 5 weeks in individual batches.

inside the chambers due to H$_2$ formation, enhancing substrate availability in the liquid phase. Then, H$_2$ accumulated was consumed at OCV mode through gas fermentation processes, which lowered the gas pressure and the bioavailability as well. The maximum acetate production rate (43.27 g m^{-2} d^{-1}) was obtained in R2 after fresh medium addition (week 4). Medium renovation could have played a role in those activities, probably due to nutrients limitation or excreted inhibitors accumulation (Ramió-Pujol et al., 2015; Rovira-Alsina et al., 2020; Vassilev et al., 2018).

3.2. A synergistic approach from the collected data

Table 1 summarizes and displays the tendency of pH, production rates, current demand, columbic efficiency (CE) and dry cell weight (DCW) for the two described reactors during the experimental period. pH decreased during repetitive weeks of power disconnection and increased once the electrical connectivity was re-established. It could be associated with the increasing accumulation of acetic acid, though the slight decline in H$_2$ production due to OCV cycles could also have influenced. Total H$_2$ production (converted + non-converted H$_2$) of R1 was higher during weeks 2 to 4 (1.24 ± 0.04 g m^{-2} d^{-1}) compared to weeks 1 and 5 (1.08 ± 0.14 g m^{-2} d^{-1}), since an increase in current demand contributed to a higher electrochemical H$_2$ formation. Moreover, higher acetate and ethanol productions were achieved (i.e. 10.81 ± 1.20 vs. 3.60 ± 3.60 g HA m^{-2} d^{-1}, respectively), which was related to a lower non-converted rate of H$_2$ (0.88 ± 0.02 vs. 0.96 ± 0.02 g m^{-2} d^{-1}, respectively). R2 followed a similar trend, but maximum H$_2$ production was attained at stable CA mode (weeks 1 and 5). The CE of both reactors improved operating at intermittent power supply, achieving the utmost value (98% in R1 and 89% in R2) when the highest acetate and H$_2$ productions were obtained. On the other hand, DCW of both reactors increased during the first week of intermittent energy supply, probably due to an effect of cell detachment. It did not reach atypical values and it

decreased once continuous energy supply was restarted. Switching electrical conditions over a relatively long period (3 weeks) could have threatened the viability of the technology (Zhang et al., 2019). However, current density gradually increased along with the experimental period, sustaining, or even exceeding production rates and conversion efficiencies.

The intermittent polarization effect (simulated using cycles of CA and OCV) was previously studied for harvesting energy from electrochemically active bacteria that usually have interrupted access to electrodes in microbial fuel cell reactors (Guo et al., 2018; Watson and Logan, 2011), even at thermophilic conditions (Carver et al., 2011). Nonetheless, understanding the mechanisms by which bacteria respond to intermittent polarization in MES can be fruitful for future energy-harvesting technologies. Although the number of MES studies in thermophilic conditions is limited and none of them operated under intermittent power supply, the values reported in this study were higher than the production rates published in the literature. Yu and co-workers obtained 3.60 g m^{-2} d^{-1} of acetate using a pure *Moorella thermoautotrophica* strain at 55 °C (Yu et al., 2017). Instead, Song et al. (2019) achieved better results using a gas diffuser in a membrane-less reactor, with a maximum acetate production of 9.61 g m^{-2} d^{-1} at 60 °C. The results of the present work were close to the maximum attained employing the same reactors as in previous tests (Rovira-Alsina et al., 2020), even surpassing acetate production rate (43.27 vs. 28.22 g m^{-2} d^{-1}). However, these outcomes are still far from other mesophilic studies such as LaBelle and May (2017) and Jourdin et al. (2015), who obtained an acetate production of 195 and 685 g m^{-2} d^{-1}, respectively. Nonetheless, they were working in galvanostatic control (83.3 A m^{-2}) and continuous CO$_2$ addition (25 mL min^{-1}) in the first case, and with a more negative potential (−0.85 V) and periodic bicarbonate addition (from 1 to 4 g L^{-1}) in the second case. Differently, Anzola Rojas and colleagues simulated possible interruptions in the renewable electricity supply by performing variable power cuts (from 4 to 64 h). Acetate
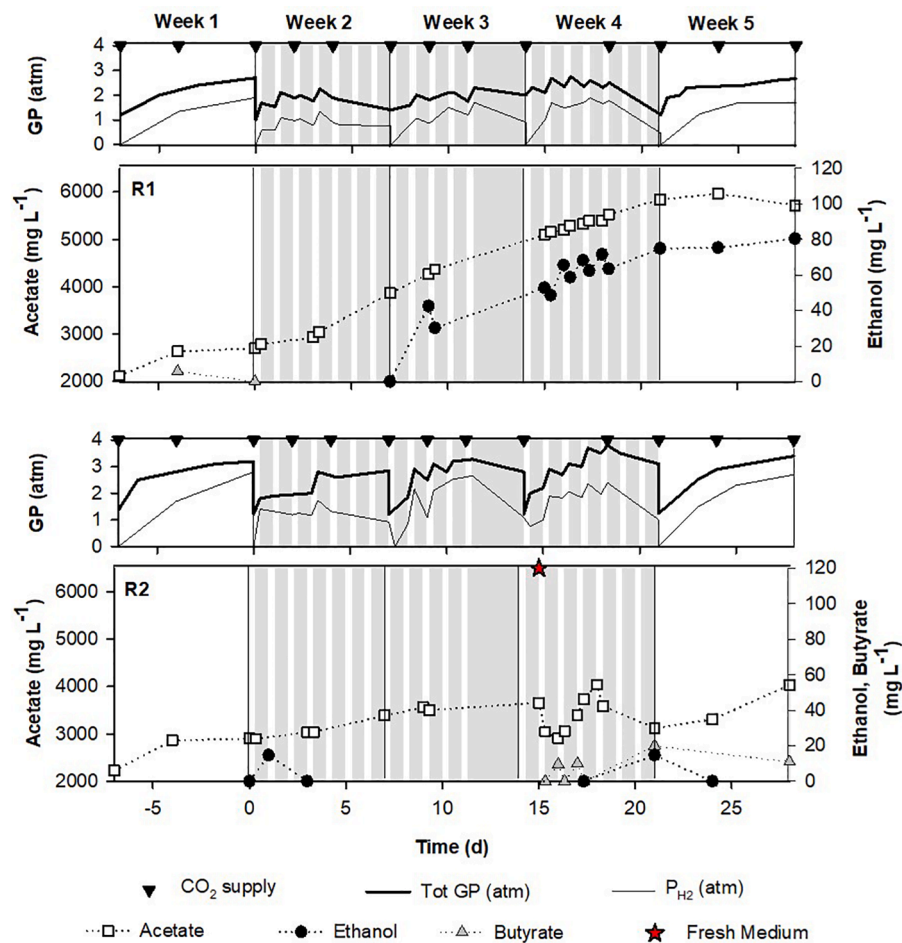
Fig. 2. Total and hydrogen partial pressure (thick and thin black lines), and more relevant organics concentration (acetate: white squares, ethanol: black circles, and butyrate: grey triangles) over time in R1 and R2. White areas represent operation at CA mode, grey areas of OCV mode, black inverted triangles the CO_2 feeding points, red star when fresh medium was added, and vertical black lines separate the 5 weeks in individual batches.

Table 1
Average pH, absolute production rates of non-converted H_2, total H_2, acetate (HA), ethanol (Et) and butyrate (HB), average current demand, columbic efficiency (CE) and dry cell weight (DCW) of R1 and R2 during the test. The tendency of each parameter throughout the 5 consecutive weeks is also displayed.

	R1						R2					
	Week 1	Week 2	Week 3	Week 4	Week 5	Tendency	Week 1	Week 2	Week 3	Week 4	Week 5	Tendency
pH	4.3 ± 0.1	4.2 ± 0.1	4.2 ± 0.1	4.1 ± 0.1	4.4 ± 0.0		6.2 ± 0.2	6.0 ± 0.3	5.9 ± 0.4	5.4 ± 0.1	5.7 ± 0.1	
H_2 (g m^{-2} d^{-1})	0.98	0.86	0.90	0.88	0.94		1.06	0.98	1.06	1.00	1.02	
Tot H_2 (g m^{-2} d^{-1})	1.18	1.26	1.26	1.21	0.98		1.30	1.15	1.09	1.20	1.28	
HA (g m^{-2} d^{-1})	6.01	12.01	10.81	10.21	1.20		7.21	5.40	3.00	43.27	9.61	
Et (g m^{-2} d^{-1})	0.00	0.00	0.49	0.30	0.06		0.00	0.00	0.00	0.16	−0.16	
HB (g m^{-2} d^{-1})	−0.06	0.00	0.00	0.00	0.00		0.00	0.00	0.00	0.21	−0.09	
Current (A m^{-2})	7.2 ± 0.5	8.2 ± 0.8	7.4 ± 0.7	8.9 ± 1.4	8.2 ± 0.3		7.5 ± 2.0	10.7 ± 1.6	11.5 ± 0.8	11.1 ± 3.3	11.9 ± 0.2	
CE (%)	51	98	98	71	20		50	72	74	89	68	
DCW (g L^{-1})	0.12	0.15	0.16	0.18	0.15		0.08	0.10	0.10	0.14	0.13	

production rate was decreased up to 77% (from 10.0 to 2.3 g m^{-2} d^{-1}) (Anzola Rojas et al., 2018b), and despite its recovery after a period of maximum 16 h, the microbial community behavior had repetitive reversions in producing-consuming acetate for its survival (Anzola Rojas et al., 2018a).

On the contrary, thermophilic microbial electrosynthesis turned out

to be a good approach to valorise renewable energy surplus converting it into organic chemicals. Our study demonstrated the capability to keep a constant production of acetate at similar rates even when electricity was deprived. The cell voltage of both reactors was increased working in discontinuous energy input (Fig. 1), which could have influenced the current demand, H_2 titer and production rates. Nevertheless, the

generation of organic compounds could be sustained throughout the experimental period (Fig. 2). Although consecutive cycles of intermittent power supply had an impact on the catalytic H_2 production, a high current density and gas pressure led to an efficient acetate production.

3.3. The tie between production slopes and reactions stoichiometry

Fig. 3 presents the evolution of pH, CO_2 and products over the week 4 of the study in R1 and R2. H_2 was produced in CA mode, but it was consumed in parallel together with CO_2 for acetate production, since under the applied potential, both reactions were thermodynamically feasible. Otherwise, fermentation processes dominated the consumption of H_2 to produce more acetate at OCV mode. Acetate production rate was lower under OCV operation, which fitted with ethanol and/or butyrate apparition. The mass balance estimated that approximately 70% of the acetate was used to produce ethanol through solventogenesis reaction, whereas butyrate could be generated through chain elongation of ethanol, or directly from acetate, H_2 and H^+ (Ganigué et al., 2015).

In R1, ethanol production was detected during OCV operation at a rate of 1.30 ± 0.47 g m^{-2} d^{-1}, whereas it was consumed at a similar velocity during CA operation (-1.40 ± 0.39 g m^{-2} d^{-1}). Meanwhile, ethanol was not detected in R2, but butyrate appeared (1.07 ± 0.03 g m^{-2} d^{-1}) and disappeared (-2.18 ± 0.081 g m^{-2} d^{-1}) during OCV and CA mode, respectively. The absence of ethanol does not imply a lack of its production, as it could have been produced and instantaneously used for butyrate synthesis (Raes et al., 2017). Under CA conditions, protons migrated from the anodic to the cathodic chamber to achieve electron neutrality (Matemadombo et al., 2016), while under OCV operation, there was still a proton diffusion, but the electron circuit transfer was cut. In concordance, pH had repetitive oscillations between cycles mainly related to the H^+ reduction during CA mode and the unceasing acetate accumulation along OCV mode. Although the slopes of H_2 and CO_2 evolution were similar among reactors, pH and the organics (acetate, ethanol and butyrate) production velocity of R1 were lower than R2. pH of R1 was closer to acetic acid pK_a at 50 °C (pK_a 4.1) which together with a high acetate concentration, favoured the shift from acetogenesis to solventogenesis (Blasco-Gómez et al., 2019), accumulating ethanol and reversing the pH tendency. Instead, pH of R2 was kept above 5. This factor together with a higher concentration of H_2 could have derived to acetate consumption for butyrate production, which was accompanied by a gradual increase in pH (Fig. 3).

Overall, carbon conversion (CC) yield from CO_2 to product for each reactor was roughly 2.3-fold higher under the span time of power supply

Table 2
Average carbon conversion yield (CC) and columbic efficiencies (CE) for R1 and R2 considering periods of power supply (CA) and disconnection (OCV).

	CC yield (%)		CE (%)			
	CA	OCV	CA		CA-OCV (batch)	
			H_{Ac}	H_2	H_{Ac}	H_2
R1	49 ± 10	20 ± 8	80 ± 5	46 ± 36	162 ± 29	56 ± 7
R2	66 ± 14	29 ± 9	46 ± 32	73 ± 24	20 ± 14	40 ± 3

(CA), coinciding with more acetate production compared to OCV mode (Table 2). About 100% of the electrons were recovered into final products when considering total H_2 production (converted + non-converted H_2), albeit R2 transformed less amount of H_2 into acetate.

3.4. Energy per product trade-off

One of the fundamental points in any catalytic system is the energy demand. Fig. 4 presents the amount of product based on the energy supplied over time. The weekly H_2 and acetate productions per unit of electrical consumption (E) were compared operating at continuous CA (weeks 1 and 5) and intermittent CA-OCV mode (weeks 2 to 4). In general, there was a gradual and concomitant growth in the ratio of product vs. energy (HA or H_2:E) within reactors. It increased over time once the cycles of intermittency begun, but it decreased when permanent electrical connectivity was re-established. That encompassed up to 138.12 g HA kWh^{-1} and 20.72 g H_2 kWh^{-1} in R1, a 18-fold higher HA:E and 7-fold higher H_2:E compared to continuous CA operation. A similar behavior was detected in R2, although the ratios were smaller as a result of lower DCW and acetate production; plus higher cell voltage and current density (Fig. 1 and Table 1).

This relationship cannot be compared to other thermophilic studies due to lack of data. However, at mesophilic conditions and CA mode, Arends et al. (2017) detailed a specific energy input per kilogram of acetic acid produced during batch processes of 29 kWh, which would be equivalent to 34.53 g HA kWh^{-1}. On the other side, Jeremiasse et al. (2010) reported an electrical energy input of 2.6 kWh per m^{-3} of H_2 formation using a Ni foam cathode, which considering the ideal gas law under normal conditions, would be equivalent to 32.02 g H_2 kWh^{-1}. Both values are within the range obtained in our experiment, though working intermittently at CA-OCV mode, the utmost HA:E proportion could exceed the previous results.
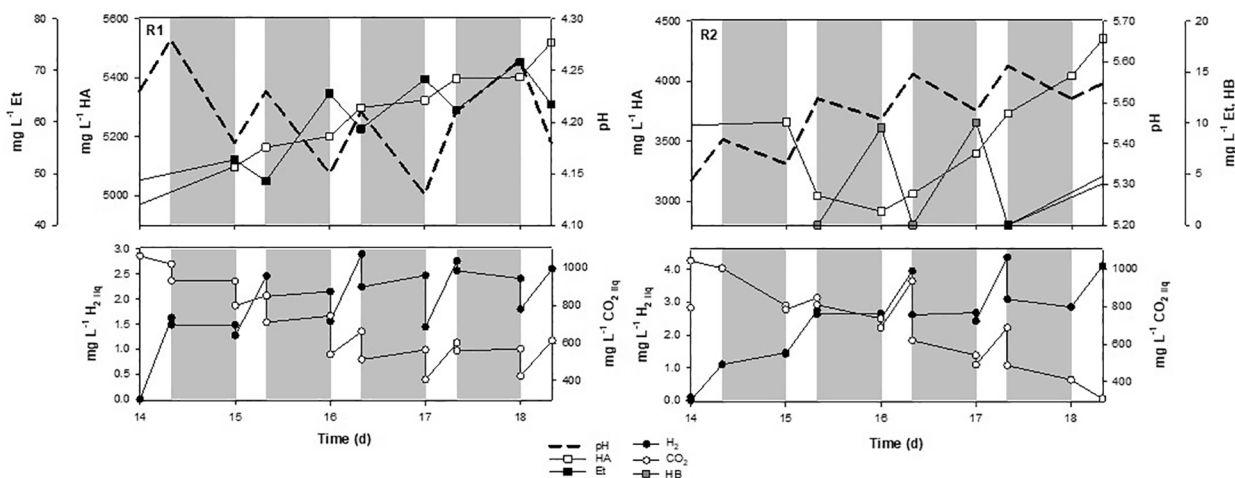
Fig. 3. Evolution of H^+ (dashed lines), ethanol (black squares), acetic acid (white squares), butyric acid (grey squares), H_2 (black circles) and CO_2 (white circles) concentrations in liquid media of R1 and R2 over the week 4 of the study. White areas represent operation at CA mode and grey areas of OCV mode. CO_2 was supplied at day 14 by oversaturating the liquid media.
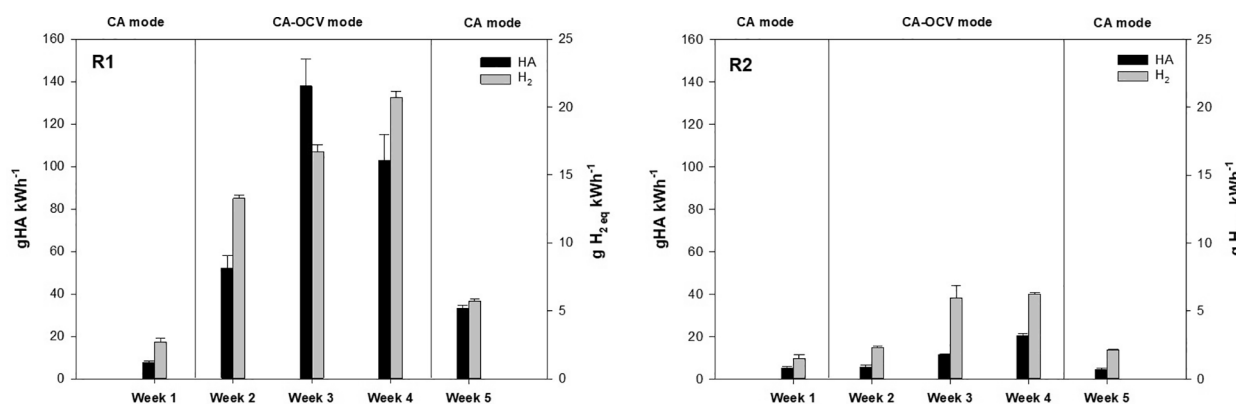
Fig. 4. Acetic acid (g HA) and H_2 (g H_2 eq) per unit of electrical energy consumption (kWh^{-1}) in each week of the analyzed period of R1 and R2.

3.5. Implications

This technology can contribute to improve the environmental pillar of sustainability and move towards a decarbonized economy by using renewable energy and CO_2 as feedstocks. 0.115 ± 0.022 kWh d^{-1} were consumed on average during the weeks before and after the assay took place (CA mode) whereas only the half, 0.056 ± 0.004 kWh d^{-1}, was required during power interruptions (CA-OCV mode) due to switching electric conditions. Although working on a laboratory scale, the total energy consumed (0.13 kWh) by R1 and R2 during the entire study (5 weeks), could save 13.31 L of natural gas, while considering the absorbed CO_2, and a CO_2 factor in Spain of 404 g kWh^{-1} (Solar edge, 2019), 53 g of CO_2 were avoided while 3 g were absorbed. This is equivalent to the amount of CO_2 that $1.6 \cdot 10^{-3}$ trees would have consumed, or differently, if applying a tree planted factor of 0.00135 trees kWh^{-1} (used in Spain), it would be equivalent to grow $1.8 \cdot 10^{-4}$ trees.

These are negligible values compared to the huge amount of energy distributed and CO_2 emitted worldwide. However, what must be considered is the impact that this technology can have if it is scaled-up to revenue excess energy and accomplish the European Union target of achieving a net-zero carbon economy by 2050 (United Nations, 2015). In order to buffer the fluctuations of naturally flowing energy, a proper strategy for storing and utilizing energy is required, and we have proposed a way to improve the efficiency of organics production from CO_2 by using intermittent power operation. However, additional experiments under different operational conditions (i.e. variable configurations and temperatures) are needed to support this premise. Increasing evidence indicates that the technology may be improved by controlling key parameters such as pH, CO_2 and H_2 through on-line probes that would allow real time monitoring for an efficient control of the process. Recently, a reactor for solar energy utilization was set up through the combination of different devices to effectively meet the demands on-site (Koike et al., 2020). In the present study, isolating H_2 and acetate productions from the organics evolution in a two-step process would allow an effective control of the main operational conditions (Ganigué et al., 2016) and therefore, the magnification of the overall productivity.

4. Conclusions

Renewable energy surplus could be valorised through thermophilic bioelectrochemical acetate production while contributing to decrease CO_2 emissions. The intermittent power connection intensified the organic compounds production: current density supplied ratio, keeping similar rates compared to continuous power operation. Bio-electro reduction of CO_2 occurred in CA mode, whereas carboxylates fermentation dominated in OCV mode. Furthermore, acetate production never ceased, as sufficient reducing power and carbon source (H_2 and CO_2, respectively) were bioavailable in any of the applied conditions. The

outcomes underscore that storing the oversupply electricity across daily cycles is a feasible challenge for the versatile MES platform.

Declaration of Competing Interest

The authors declare that they have no known competing financial interests or personal relationships that could have appeared to influence the work reported in this paper.

Appendix A. Supplementary data

Supplementary data to this article can be found online at https://doi.org/10.1016/j.biortech.2020.124423.

References

Anvari, M., Lohmann, G., Wächter, M., Milan, P., Lorenz, E., Heinemann, D., Tabar, M.R. R., Peinke, J., 2016. Short term fluctuations of wind and solar power systems. New J. Phys. 18 https://doi.org/10.1088/1367-2630/18/6/063027.

Anzola Rojas, M. del P., Mateos, R., Sotres, A., Zaiat, M., Gonzalez, E.R., Escapa, A., De Wever, H., Pant, D., 2018a. Microbial electrosynthesis (MES) from CO2 is resilient to fluctuations in renewable energy supply. Energy Convers. Manag. 177, 272–279. https://doi.org/10.1016/j.enconman.2018.09.064.

Anzola Rojas, M. del P., Zaiat, M., Rafael, E., Wever, H. De, 2018b. Effect of the electric supply interruption on a microbial electrosynthesis system converting inorganic carbon into acetate. Bioresour. Technol. 266, 203–210. https://doi.org/10.1016/j.biortech.2018.06.074.

Arends, J.B.A., Patil, S.A., Roume, H., Rabaey, K., 2017. Continuous long-term electricity-driven bioproduction of carboxylates and isopropanol from CO2 with a mixed microbial community. J. CO2 Util. 20, 141–149. https://doi.org/10.1016/j.jcou.2017.04.014.

Batlle-Vilanova, P., Rovira-Alsina, L., Puig, S., Balaguer, M.D., Icaran, P., Monsalvo, V. M., Rogalla, F., Colprim, J., 2019. Biogas upgrading, CO2 valorisation and economic revaluation of bioelectrochemical systems through anodic chlorine production in the framework of wastewater treatment plants. Sci. Total Environ. 690, 352–360. https://doi.org/10.1016/j.scitotenv.2019.06.361.

Bian, B., Bajracharya, S., Xu, J., Pant, D., Saikaly, P.E., 2020. Microbial electrosynthesis from CO2: Challenges, opportunities and perspectives in the context of circular bioeconomy. Bioresour. Technol. 302, 122863 https://doi.org/10.1016/j.biortech.2020.122863.

Blasco-Gómez, R., Ramió-Pujol, S., Baneras, L., Colprim, J., Balaguer, M.D., Puig, S., 2019. Unravelling the factors that influence the bio-electrorecycling of carbon dioxide towards biofuels. Green Chem. 21, 684–691. https://doi.org/10.1039/C8GC03417F.

Carver, S.M., Vuoriranta, P., Tuovinen, O.H., 2011. A thermophilic microbial fuel cell design. J. Power Sources 196, 3757–3760. https://doi.org/10.1016/j.jpowsour.2010.12.088.

Ceballos-Escalera, A., Molognoni, D., Bosch-Jimenez, P., Shahparasti, M., Bouchakour, S., Luna, A., Guisasola, A., Borràs, E., Della Pirriera, M., 2019. Bioelectrochemical systems for energy storage: A scaled-up power-to-gas approach. Appl. Energy 260, 114138. https://doi.org/10.1016/j.apenergy.2019.114138.

Denchak, M., 2018. Fossil Fuels: The Dirty Facts. URL https://www.nrdc.org/stories/fossil-fuels-dirty-facts (accessed 9.24.19).

Energy research Centre of the Netherlands, 2011. Cost-Efficient and Sustainable Deployment of Renewable Energy Sources towards the 20% Target by 2020, and beyond.

European Environment Agency Share of renewable energy in gross final energy consumption in Europe https://www.eea.europa.eu/data-and-maps/indicators/renewable-gross-final-energy-consumption-4/assessment-4 2019 accessed 5.6.20.

Foust, A.S., Wenzel, L.A., Maus, L., Andersen, L.B., 1959. Principles of Unit Operations. Wiley Int. Ed. 369–400.

Ganigué, R., Puig, S., Batlle-Vilanova, P., Balaguer, M.D., Colprim, J., 2015. Microbial electrosynthesis of butyrate from carbon dioxide. Chem. Commun. 51, 3235–3238. https://doi.org/10.1039/c4cc10121a.

Ganigué, R., Sánchez-Paredes, P., Bañeras, L., Colprim, J., 2016. Low fermentation pH is a trigger to alcohol production, but a killer to chain elongation. Front. Microbiol. 7, 1–11. https://doi.org/10.3389/fmicb.2016.00702.

Gowrisankaran, G., Reynolds, S.S., Samano, M., 2015. Intermittency and the value of renewable energy. J. Chem. Inf. Model. 53, 1689–1699. https://doi.org/10.1017/CBO9781107415324.004.

Grim, R.G., Huang, Z., Guarnieri, M.T., Ferrell, J.R., Tao, L., Schaidle, J.A., 2020. Transforming the carbon economy: challenges and opportunities in the convergence of low-cost electricity and reductive CO 2 utilization. Energy Environ. Sci. 13, 472–494. https://doi.org/10.1039/c9ee02410g.

Guo, F., Babauta, J.T., Beyenal, H., 2018. Impact of intermittent polarization on electrode-respiring Geobacter sulfurreducens biofilms. J. Power Sources 406, 96–101. https://doi.org/10.1016/j.jpowsour.2018.10.053.

Hu, X., Zou, C., Zhang, C., Li, Y., 2017. Technological developments in batteries: a survey of principal roles, types, and management needs. IEEE Power Energy Mag. 15, 20–31. https://doi.org/10.1109/MPE.2017.2708812.

Jadhav, D.A., Chendake, A.D., Schievano, A., Pant, D., 2018. Suppressing methanogens and enriching electrogens in bioelectrochemical systems. Bioresour. Technol. https://doi.org/10.1016/j.biortech.2018.12.098.

Jeremiasse, A.W., Hamelers, H.V.M., Saakes, M., Buisman, C.J.N., 2010. Ni foam cathode enables high volumetric H2 production in a microbial electrolysis cell. Int. J. Hydrogen Energy 35, 12716–12723. https://doi.org/10.1016/j.ijhydene.2010.08.131.

Jourdin, L., Grieger, T., Monetti, J., Flexer, V., Freguia, S., Lu, Y., Chen, J., Romano, M., Wallace, G.G., Keller, J., 2015. High acetic acid production rate obtained by microbial electrosynthesis from carbon dioxide. Environ. Sci. Technol. 49, 13566–13574. https://doi.org/10.1021/acs.est.5b03821.

Jourdin, L., Winkelhorst, M., Rawls, B., Buisman, C.J.N., Strik, D.P.B.T.B., 2019. Enhanced selectivity to butyrate and caproate above acetate in continuous bioelectrochemical chain elongation from CO2: Steering with CO2 loading rate and hydraulic retention time. Bioresour. Technol. Reports 7, 100284. https://doi.org/10.1016/j.biteb.2019.100284.

Koike, K., Fujii, K., Kawano, T., Wada, S., 2020. Bio-mimic energy storage system with solar light conversion to hydrogen by combination of photovoltaic devices and electrochemical cells inspired by the antenna-associated photosystem II. Plant Signal. Behav. 00 https://doi.org/10.1080/15592324.2020.1723946.

LaBelle, E.V., May, H.D., 2017. Energy efficiency and productivity enhancement of microbial electrosynthesis of acetate. Front. Microbiol. 8, 1–9. https://doi.org/10.3389/fmicb.2017.00756.

Liu, Z., Wang, K., Chen, Y., Tan, T., Nielsen, J., 2020. Third-generation biorefineries as the means to produce fuels and chemicals from CO2. Nat. Catal. 3 https://doi.org/10.1038/s41929-019-0421-5.

Matemadombo, F., Puig, S., Ganigué, R., Ramírez-García, R., Batlle-Vilanova, P., Balaguer, M., Colprim, J., 2016. Modelling the simultaneous production and separation of acetic acid from CO2 using an anion exchange membrane microbial electrosynthesis system. Chem. Technol. Biotechnol. 92, 1211–1217. https://doi.org/10.1002/jctb.5110.

Nevin, K.P., Woodard, T.L., Franks, A.E., 2010. Microbial Electrosynthesis : Feeding Microbes Electricity To Convert Carbon Dioxide and Water to Multicarbon

Extracellular Organic. Am. Soc. Microbiol. 1, 1–4. https://doi.org/10.1128/mBio.00103-10.Editor.

Patil, S.A., Gildemyn, S., Pant, D., Zengler, K., Logan, B.E., Rabaey, K., 2015. A logical data representation framework for electricity-driven bioproduction processes. Biotechnol. Adv. 33, 736–744. https://doi.org/10.1016/j.biotechadv.2015.03.002.

Pepè Sciarria, T., Batlle-Vilanova, P., Colombo, B., Scaglia, Barbara, Balaguer, M.D., Colprim, J., Puig, S., Adani, Fabrizio, 2018. Bio-electrorecycling of carbon dioxide into bioplastics. Green Chem. https://doi.org/10.1039/C8GC01771A.

Puig, S., Ganigué, R., Batlle-Vilanova, P., Balaguer, M.D., Bañeras, L., Colprim, J., 2017. Tracking bio-hydrogen-mediated production of commodity chemicals from carbon dioxide and renewable electricity. Bioresour. Technol. 228, 201–209. https://doi.org/10.1016/j.biortech.2016.12.035.

Rabaey, K., Rozendal, R.A., 2010. Microbial electrosynthesis - Revisiting the electrical route for microbial production. Nat. Rev. Microbiol. 8, 706–716. https://doi.org/10.1038/nrmicro2422.

Raes, S.M.T., Jourdin, L., Buisman, C.J.N., Strik, D.P.B.T.B., 2017. Continuous long-term bioelectrochemical chain elongation to butyrate. ChemElectroChem 4, 386–395. https://doi.org/10.1002/celc.201600587.

Ramió-Pujol, S., Ganigué, R., Bañeras, L., Colprim, J., 2015. Incubation at 25°C prevents acid crash and enhances alcohol production in Clostridium carboxidivorans P7. Bioresour. Technol. 192, 296–303. https://doi.org/10.1016/j.biortech.2015.05.077.

Rovira-Alsina, L., Perona-Vico, E., Bañeras, L., Colprim, J., Balaguer, M.D., Puig, S., 2020. Thermophilic bio-electro CO2 recycling into organic compounds. Green Chem. 22, 2947–2955. https://doi.org/10.1039/d0gc00320d.

Roy, M., Yadav, R., Chiranjeevi, P., Patil, S.A., 2021. Direct utilization of industrial carbon dioxide with low impurities for acetate production via microbial electrosynthesis. Bioresour. Technol. 320, 124289 https://doi.org/10.1016/j.biortech.2020.124289.

Sánchez, O.G., Birdja, Y.Y., Bulut, M., Vaes, J., Breugelmans, T., Pant, D., 2019. Recent advances in industrial CO2 electroreduction. Opin. Green Sustain. Chem. Curr. https://doi.org/10.1016/j.cogsc.2019.01.005.

Solar edge, 2019. Technical Note – Monitoring Platform Environmental Benefits Calculation.

Song, H., Choi, O., Pandey, A., Kim, Y.G., Joo, J.S., Sang, B.I., 2019. Simultaneous production of methane and acetate by thermophilic mixed culture from carbon dioxide in bioelectrochemical system. Bioresour. Technol. 281, 474–479. https://doi.org/10.1016/j.biortech.2019.02.115.

Spanish solar radiation data. URL http://www.adrase.com/en/ (accessed 10.3.19).

Streeck, J., Hank, C., Neuner, M., Gil-Carrera, L., Kokko, M., Pauliuk, S., Schaadt, A., Kerzenmacher, S., White, R.J., 2018. Bio-electrochemical conversion of industrial wastewater combined with downstream methanol synthesis – an economic- and life cycle assessment. Green Chem. 00, 1–3. https://doi.org/10.1039/C8GC00543E.

Stumm, W., Morgan, J.J., 1996. Aquatic chemistry – chemical equilibria and rates in natural waters. Environ. Sci. Technol.

Tanner, R.S., Miller, L.M., Yang, D., 1993. Clostridium ljungdahlii sp. nov., an acetogenic species in clostridial rRNA homology group I. Int. J. Syst. Bacteriol. 43, 232–236. https://doi.org/10.1099/00207713-43-2-232.

United Nations, 2015. Paris agreement.

Vassilev, I., Hernandez, P.A., Batlle-Vilanova, P., Freguia, S., Krömer, J.O., Keller, J., Ledezma, P., Virdis, B., 2018. Microbial electrosynthesis of isobutyric, butyric, caproic acids, and corresponding alcohols from carbon dioxide. ACS Sustain. Chem. Eng. 6, 8485–8493. https://doi.org/10.1021/acssuschemeng.8b00739.

Vassilev, I., Kracke, F., Freguia, S., Keller, J., Krömer, J.O., Ledezma, P., Virdis, B., 2019. Microbial electrosynthesis system with dual biocathode arrangement for simultaneous acetogenesis, solventogenesis and carbon chain elongation. Chem. Commun. 55, 4351–4354. https://doi.org/10.1039/c9cc00208a.

Watson, V.J., Logan, B.E., 2011. Analysis of polarization methods for elimination of power overshoot in microbial fuel cells. Electrochem. Commun. 13, 54–56. https://doi.org/10.1016/j.elecom.2010.11.011.

WEO, 2018. The gold standard of energy analysis. accessed 9.24.19. https://www.iea.org/weo2018/.

Yu, L., Yuan, Y., Tang, J., Zhou, S., 2017. Thermophilic Moorella thermoautotrophica-immobilized cathode enhanced microbial electrosynthesis of acetate and formate from CO2. Bioelectrochemistry 117, 23–28. https://doi.org/10.1016/j.bioelechem.2017.05.001.

Zhang, X., Rabaey, K., Prévoteau, A., 2019. Reversible effects of periodic polarization on anodic electroactive biofilms. ChemElectroChem 6, 1921–1925. https://doi.org/10.1002/celc.201900228.